

A photoionization study of the vinyl radical

J. Berkowitz, C. A. Mayhew, and B. Rušćić^{a)}

Chemistry Division, Argonne National Laboratory, Argonne, Illinois 60439

(Received 17 November 1987; accepted 13 January 1988)

The photoionization spectrum of vinyl radical is reported, from its observed threshold to 1160 Å. Two methods of preparation have been employed; (a) the abstraction reaction of F atoms with C₂H₄, and (b) the pyrolysis of divinyl mercury at 1200 K. In both experiments, relatively sharp autoionization structure is observed, and interpreted as a Rydberg series converging to the excited ³A' state of vinyl cation. The analysis leads to an adiabatic ionization energy of ~10.7 eV for this state, with a structure similar to that of vinyl radical but with an increased C–C distance. The observed ionization threshold for the ground state of vinyl cation is 8.59 ± 0.03 eV with the F atom reaction, and 8.43 ± 0.03 eV with the pyrolysis method. The lower value in the latter experiment is interpreted as a hot band. The relatively low value of the photoionization cross section near threshold implies a large geometry change between vinyl radical and ground state vinyl cation. A progression in the in-plane C–H bending vibration is indicated in the photoionization spectrum; it is quite possible that the vibrational 0–0 transition lies one quantum lower than our detected limit. With this bracketed adiabatic ionization potential and the appearance potential of C₂H₃⁺ (C₂H₄), a C–H bond energy in ethylene of 107–110 kcal/mol (0 K) is deduced.

I. INTRODUCTION

Two topics currently receiving considerable attention in the chemical physics community are: (1) the heat of formation of the vinyl radical (or almost equivalently, the C–H bond energy in ethylene) and (2) the molecular geometry of the ground state of the vinyl cation.

A. Energetics

Since $\Delta H_f^0(\text{H})$ and $\Delta H_f^0(\text{C}_2\text{H}_4)$ are well-known quantities,¹ we can provide a relationship between $\Delta H_f(\text{C}_2\text{H}_3)$ and ΔH_{BE} (where ΔH_{BE} is the C–H bond energy in C₂H₄) with some confidence. Thus,

$$\Delta H_{\text{BE},0} = \Delta H_f^0(\text{C}_2\text{H}_3) + 37.05 \text{ kcal/mol}$$

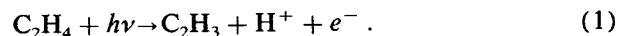
and

$$\Delta H_{\text{BE},298} = \Delta H_{f,298}^0(\text{C}_2\text{H}_3) + 39.56 \text{ kcal/mol},$$

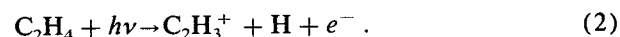
with an uncertainty of ± 0.07 kcal/mol.

Recently, Shiromaru *et al.*² have reported a value of 5.06 ± 0.05 eV ≡ 116.7 ± 1.2 kcal/mol for $\Delta H_{\text{BE},0}$, equivalent to $\Delta H_f^0(\text{C}_2\text{H}_3) = 79.7 \pm 1.2 \text{ kcal/mol}$.

This result was based on a measured threshold of 18.66 ± 0.05 eV for the reaction



This photoionization experiment, performed with synchrotron radiation, was reported² to have had difficulty excluding second-order radiation. Prior photoionization studies relevant to the present discussion had focused on the process



Three measurements of the threshold have been reported

for this process, 13.80,³ 13.25 ± 0.05,⁴ and 13.22 ± 0.02⁵ eV. These values can be related to corresponding ones for $\Delta H_f^0(\text{C}_2\text{H}_3^+) = 281.1, 268.4 \pm 1.2,$ and $267.8 \pm 0.5 \text{ kcal/mol}$, respectively. Reinke *et al.*⁶ have studied the photoionization threshold for C₂H₃⁺ from C₂H₃Cl, and deduced $\Delta H_{f,298}^0(\text{C}_2\text{H}_3^+) = 264 \pm 2 \text{ kcal/mol}$, which can be converted to $\Delta H_f^0(\text{C}_2\text{H}_3^+) = 265 \pm 2 \text{ kcal/mol}$ from available thermochemical data.⁷ Thus, it seems plausible to conclude that $\Delta H_f^0(\text{C}_2\text{H}_3^+)$ lies between 265–269 kcal/mol, and that the earliest photoionization result³ is in error.

In order to deduce ΔH_{BE} or $\Delta H_f^0(\text{C}_2\text{H}_3)$ from such an experiment, one must know the adiabatic ionization potential of vinyl radical. In earlier work, Harrison and Lossing⁸ used conventional electron impact mass spectrometry on vinyl radical produced by the pyrolysis of methylvinyl mercury, and obtained 9.45 eV. Later, Lossing⁹ used an energy-resolved electron beam on vinyl radical generated by pyrolysis of divinyl sulfone, and obtained 8.95 eV. This latter value has been selected in the compilation by Rosenstock *et al.*,¹⁰ and they also choose $\Delta H_f^0(\text{C}_2\text{H}_3^+) = 269 \text{ kcal/mol}$. This latter set of data is equivalent to $\Delta H_{\text{BE},0} = 99.7 \text{ kcal/mol}$ and $\Delta H_f^0(\text{C}_2\text{H}_3) = 62.6 \text{ kcal/mol}$, each about 17 kcal/mol lower than the corresponding recent values of Shiromaru *et al.*²

Appearance potential measurements, by their very nature, give upper limits to the energy threshold for a particular process. Hence, it might be argued that the threshold for C₂H₃⁺ (C₂H₄) is also just an upper limit, and not a valid thermochemical threshold. Independent support for the view that this is a thermochemically significant threshold has recently been provided by two extensive *ab initio* calculations^{11,12} of the proton affinity of acetylene, defined as the exothermicity of the process



^{a)} Also Physical Chemistry Department, Rugjer Bošković Institute, Zagreb, Yugoslavia.

Lindh *et al.*¹¹ report 154.8 kcal/mol, while Curtiss and Pople obtain 152.5 kcal/mol, at 0 K. The range of values for $\Delta H_f^0(\text{C}_2\text{H}_3^+)$ we have selected (265–269 kcal/mol) correspond to a range 154.6–150.6 kcal/mol for the proton affinity of C_2H_2 at 0 K. The value obtained from the *ab initio* calculations of Lindh *et al.* favors the lower end of our range for $\Delta H_f^0(\text{C}_2\text{H}_3^+)$, whereas the value calculated by Curtiss and Pople comes very close to the value (151.8 kcal/mol) deduced from the experiment of Stockbauer and Inghram,⁵ which has the highest precision of the experimental thresholds.

Hence, of the two quantities entering into the determination of the lower values of ΔH_{BE} and $\Delta H_f(\text{C}_2\text{H}_3)$, the one most suspect is almost certainly the ionization potential of vinyl radical. This problem is avoided in the measurement of Shiromaru *et al.*,² since the ionization potential of atomic hydrogen is perhaps the best known thermochemical quantity. However, there are other possible criticisms of this measurement. The H^+ signal is weak, and these authors recognize problems with second-order radiation. In addition, there is the likelihood of a kinetic shift. In the photodissociation of ethylene,^{4,5} lower energy processes occur at 13.13 ± 0.02 eV ($\text{C}_2\text{H}_2^+ + \text{H}_2$), 13.25 eV ($\text{C}_2\text{H}_3^+ + \text{H}$), and ~ 18.05 eV ($\text{CH}_2^+ + \text{CH}_2$) before the desired process ($\text{H}^+ + \text{C}_2\text{H}_3$) begins to be seen at 18.66 ± 0.05 eV. In the language of unimolecular decay theory, the phase space, and hence rate of decomposition of the lower energy processes is very large at the thermochemical onset of H^+ . The rate of the latter process is low at threshold. If these processes are in competition with one another, the phase space for the H^+ producing process must increase (i.e., energy beyond threshold must be added) before it attains an observable rate. One such example is the threshold for CH_3^+ from C_2H_6 , which has a thermochemical onset at 13.586 eV, but is first observed at ~ 13.96 eV.¹³ If there is a substantial kinetic shift in the $\text{H}^+ + \text{C}_2\text{H}_3$ threshold, it would result in too large a value for ΔH_{BE} , and also for $\Delta H_f^0(\text{C}_2\text{H}_3)$.

When faced with such disparate values, and with arguments for questioning both results, one can examine the deductions from other methods to provide a basis for judgment. Thus, McMillen and Golden¹⁴ select $\Delta H_{f,298}^0(\text{C}_2\text{H}_3) = 70.4 \pm 2$ kcal/mol, and $\Delta H_{\text{BE},298} = 110 \pm 2$ kcal/mol, based largely on kinetic methods. However, a more recent kinetic study by Kieffer *et al.*¹⁵ leads to $\Delta H_{f,298}^0(\text{C}_2\text{H}_3) = 63.4 \pm 2$ kcal/mol, which is essentially the same as the low value obtained from photoionization.

Shiromaru *et al.*² cite an unpublished value [A. M. Wodtke, E. J. Hints, I. Dubourg, and Y. T. Lee (to be submitted)] of 4.71 eV \equiv 108.6 kcal/mol for $\Delta H_{\text{BE},0}$ from the analysis of the photofragment translational spectra of $\text{C}_2\text{H}_3\text{Br}$ and the translational energy release in the $\text{F} + \text{C}_2\text{D}_4 \rightarrow \text{C}_2\text{D}_3 + \text{DF}(v=4)$ reaction. This value of $\Delta H_{\text{BE},0}$ implies $\Delta H_f^0(\text{C}_2\text{H}_3) = 71.6$ kcal/mol, which is consistent with the aforementioned selection of McMillen and Golden.¹⁴ Finally, Ellison¹⁶ has recently obtained $\Delta H_{\text{BE},298} = 107.8 \pm 3.1$ kcal/mol by combining his determination¹⁷ of the electron affinity of C_2H_3 with an indirectly determined gas phase acidity for C_2H_3 . These alternative values are listed for convenience in Table I. In summary, the

TABLE I. Summary of values for $\Delta H_f^0(\text{C}_2\text{H}_3)$, $\Delta H_f^0(\text{C}_2\text{H}_3^+)$ and $\Delta H_{\text{BE},0}$ (all in kcal/mol) from various sources.

$\Delta H_f^0(\text{C}_2\text{H}_3)^a$	$\Delta H_f^0(\text{C}_2\text{H}_3^+)$	$\Delta H_{\text{BE},0}$	Ref.
	281.1		3
	268.4 ± 1.2		4
	267.8 ± 0.5		5
	265 ± 2		6
62.6	269	99.7	10
71.5 ± 2		108.6 ± 2	14
64.5 ± 2		101.6 ± 2	15
79.7 ± 1.2		116.7 ± 1.2	2
71.6		108.6	WHDL ^b
70.4		107.4 ± 3.1	16 ^c
71.9		108.9 ± 2	12
> 69.8		> 106.8	Present
70-73		107-110	results

^a In order to reduce the number of cited values at 298 and at 0 K, we have converted all values to 0 K using $\Delta H_f^0(\text{C}_2\text{H}_3) = \Delta H_{f,298}^0(\text{C}_2\text{H}_3) + 1.1$ kcal/mol given in Ref. 7, and also related $\Delta H_{\text{BE},0}$ to $\Delta H_f^0(\text{C}_2\text{H}_3)$ using Eq. (1).

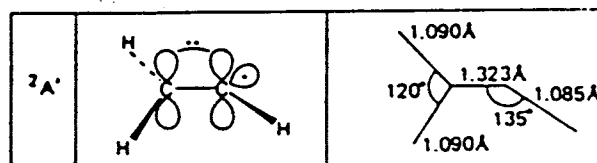
^b WHDL = Wodtke, Hints, Dubourg, and Lee, cited in Ref. 2.

^c This value, slightly different from that given by Ref. 16, utilizes the correction to 0 K given in footnote a.

values for ΔH_{BE} inferred from other methods cluster around an intermediate value of 108–110 kcal/mol, except for a recent kinetic result that yields ~ 102 kcal/mol. None approach the high photoionization value of 117 kcal/mol.

B. Molecular geometry

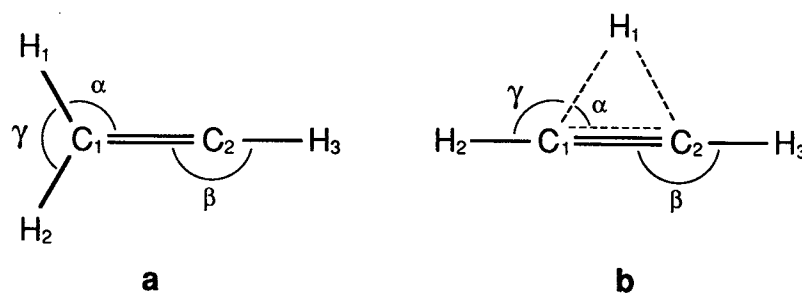
Recent experiments and *ab initio* SCF calculations¹⁸ have led to the conclusion that the ground state of vinyl radical has a planar, ethylene-like structure, as shown below.



Much more attention has been focused on the potential surface of the ground state of vinyl cation. The results of three recent, extensive *ab initio* calculations^{11,19,20} are summarized in Table II. It can readily be seen from this table that the three groups are in general agreement about the molecular geometry of the two structures, which are often referred to as the classical and nonclassical (bridged) structure. They differ somewhat with regard to the detailed potential surface. Curtiss and Pople's¹² most recent calculation places the classical structure 3.1 kcal/mol above (i.e., less stable than) the nonclassical structure with a barrier between them²⁰ of at most 0.3 kcal/mol, and perhaps zero (i.e., the classical structure is a saddle point on the surface). Lindh *et al.*¹¹ have the classical structure 3.6–4.1 kcal/mol above the nonclassical structure, with a barrier of 0.7 kcal/mol. Lee and Schaeffer¹⁹ compute that the classical structure is 1–1.5 kcal/mol less stable, including zero point energy effects.

Recent experiments also tend to favor the bridged, nonclassical structure as being the most stable one for vinyl cation. Oka²¹ has assigned a number of lines in the infrared

TABLE II. Calculated molecular geometries of (a) the classical and (b) the nonclassical (bridged) structures of vinyl cation.



	α	$R_{CC}, \text{\AA}$	$R_{C,H_1}, \text{\AA}$	$R_{C,H_2}, \text{\AA}$	$R_{C,H_3}, \text{\AA}$	β	γ
LS ^a (a)	120.3°	1.275	1.098	1.098	1.087	180°	119.5°
P ^b (a)	121.0°	1.262	1.101	1.101	1.084	180°	118°
LRK ^c (a)	120.42°	1.266	1.116	1.116	1.098	180°	119.2°
LS (b)	61.7°	1.234	1.281	1.084	1.084	179.8	118.6
P (b)	61.1°	1.232	1.276	1.081	1.081	180.3	118.6
LRK (b)	61.74°	1.227	1.296	1.096	1.096	179.1	119.1

^aLS = Lee and Schaeffer, Ref. 19. ^bP = Pople, Ref. 20. ^cLRK = Lindh, Roos, and Kraemer, Ref. 11.

spectrum of a discharge in a $C_2H_2-H_2$ mixture. From these assignments, he has obtained rotational constants which are in good agreement with those predicted by Lee and Schaeffer,¹⁹ and presumably the other calculations listed in Table II. However, he notes that, "while these results establish the carrier of the spectrum to be $C_2H_3^+$ with the nonclassical structure dominating ... there are various indications that the spectrum is not that of a usual well behaved asymmetric rotor." He states that his "... observations may be associated with the proton tunneling expected from the theoretically calculated small energy difference between the nonclassical and classical ions and the small barrier separating them." A quite different experiment, referred to as the Coulomb explosion technique,²² has led to the conclusion that the average geometry corresponds to the nonclassical structure.

If vinyl radical has the ethylene-like structure shown above, and vinyl cation has the bridged, nonclassical structure, then photoionization of vinyl radical should be extremely weak at threshold, since the large change in geometry should result in very unfavorable Franck-Condon factors near the adiabatic ionization threshold.

Thus, our undertaking of a study of the photoionization of vinyl radical has two goals, which can be anticipated to be difficult to achieve: (a) a measurement of the adiabatic ionization potential of C_2H_3 , from which one may extract $\Delta H_f^0(C_2H_3^+)$ and ΔH_{BE} , and (b) an analysis of the energy dependence of the photoion yield curve near threshold, from which one might hope to extract some information about the potential surface of the ground state of vinyl cation, and hence its geometry.

II. EXPERIMENTAL ARRANGEMENT

The basic photoionization mass spectrometric apparatus has been described previously.^{23(a)}

Two rather different procedures were used to generate

vinyl radical in a steady state. The first was the reaction of F atoms with C_2H_4 . This reaction proceeds primarily by substitution ($C_2H_3F + H$), and in fact, the dynamics of this pathway have been studied extensively.²⁴ However, the abstraction reaction ($C_2H_3 + HF$) accounts for about 25%–35% of the products.^{24,25} Bogan and Setser²⁶ have measured the energy disposal in this abstraction reaction, as well as reviewing earlier work. It seems as if most of the exothermicity in this reaction manifests itself in vibrational excitation of HF.^{24,26} This observation conforms with our previous experience with such abstraction reactions where we have concluded that the radicals generated leave the reaction chamber with an internal energy distribution corresponding to room temperature. The reactor used for generating C_2H_3 is identical to the device employed for producing SiH_n radicals.^{23(b)} Fluorine atoms, produced in a microwave discharge through pure F_2 , flow rapidly through a delivery tube. A small fraction enter a reaction cup, to which C_2H_4 has been introduced. After a few collisions, the product species effuse through an orifice and enter the photoionization chamber. The fast-flowing fluorine is removed by a cryopump.

The second method of producing C_2H_3 was by pyrolysis of $(C_2H_3)_2Hg$ at a temperature of ~ 1200 K. The pyrolysis reactor employed is identical to the one used in recent pyrolysis experiments on benzyl phosphine.²⁷ In earlier work, Lossing⁸ used methylvinyl mercury pyrolysis as a source of C_2H_3 , but subsequently reported⁹ that, "... the radicals were obtained more conveniently and in somewhat better yield from the pyrolysis of divinyl sulfone." As a consequence, we began our pyrolysis studies with divinyl sulfone, but discovered that the yield was not high, and it was irregular. Divinyl mercury proved to be a more satisfactory precursor. Since $C_2H_3^+$ is a fragment from dissociative ionization of cold divinyl mercury, it was necessary to study this photoion yield curve in order to establish an energy region for primary ionization of C_2H_3 uncontaminated by the dissociative ioniza-

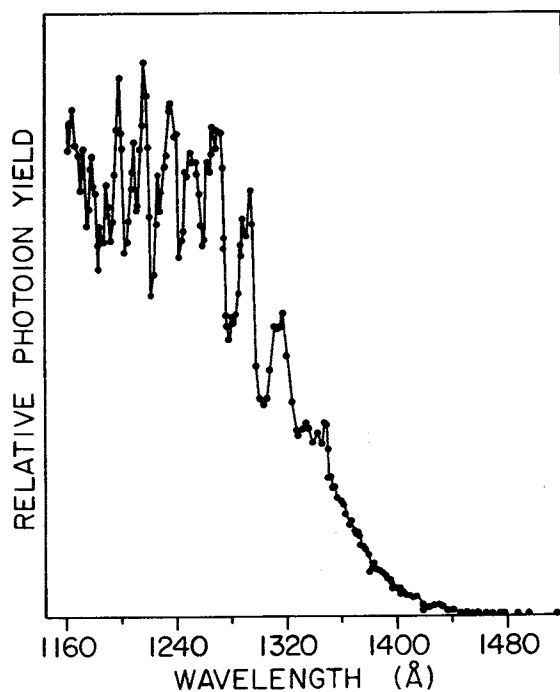


FIG. 1. Overview spectrum of the photoion yield of $C_2H_3^+$ (C_2H_3), where C_2H_3 is prepared by the $F + C_2H_4$ reaction.

tion process. In the course of this study, we obtained the photoion yield curves of parent and major fragment ions from divinyl mercury, which we also report below.

Since the ion signals were weak, especially in the region near threshold, most of the experiments were conducted using only the peak light intensities in the many-line spectrum of molecular hydrogen.

III. EXPERIMENTAL RESULTS AND INTERPRETATION

A. C_2H_3 from $F + C_2H_4$ reaction

An overview of this photoion yield curve of $C_2H_3^+$ (C_2H_3) is shown in Fig. 1. The most prominent features of this spectrum are the rather large autoionization resonances. The wavelengths at the peaks of these resonances are listed in Table III. Such structure is common in the photoionization of atoms, diatomic, and sometimes triatomic molecules, but not so common for larger molecules. For example, C_2H_2 has weak autoionization structure,¹³ and structure is barely perceptible¹³ in C_2H_4 . The resonances, superposed upon a relatively intense ionization continuum, span the region from ~ 1200 – 1350 Å. To longer wavelength, the photoion yield curve descends rather quickly, in what appear to be step-like features with intervals of ~ 7.5 Å (400 cm^{-1}) until about 1400 Å. At still longer wavelengths, the cross section varies more slowly, and appears to reach the background level at about 1450 Å. Even this cursory view is sufficient to establish that Lossing's⁹ ionization potential of $8.95\text{ eV} \equiv 1385$ Å is too high. Also, the first differential of his electron impact ionization curve, which could conceivably mimic the photoionization curve, does not bear any significant resemblance to Fig. 1.

The relatively slow ascent of the photoion yield curve from threshold to ~ 1400 Å suggests, but does not prove, a large change in geometry between vinyl radical and the

TABLE III. Wavelengths (Å) of the peaks of the autoionization resonances in the photoionization of vinyl radical.

C_2H_3 ($F + C_2H_4$)	C_2H_3 (Pyrolysis)
1347.3	1347.5
1342.3	1342.0
1333.7	1333.8
1316.5	1315.6
1310.9	
1293.3	1292.9
1287.7	1289.4
1271.4	1271.7
1268.9	1268.7
1265.7	1265.5
	1255.0
1250.4	1249.6
1248.8	
1235.5	
1234.1	1233.9
1215.6	1215.4
1208.9	1208.7
1197.7	1197.5
1188.4	1188.1
1178.2	1178.1
1171.9 (?)	
	1169.4 (?)
1163.8 (?)	

ground state of the cation. An alternative explanation is that the quantum yield of ionization increases gradually from threshold. We shall return to this important question, the interpretation of threshold behavior, in a subsequent section. For the moment, we shall consider in greater detail the resonance region.

According to Hunziker *et al.*,¹⁸ the orbital sequence of vinyl radical in its ground state can be written as

$$(1a')^2 \cdots (6a')^2 (7a') (1a'')^2, {}^2A'$$

The singlet ground state of the cation is formed when the electron in the singly occupied $7a'$ orbital is ejected. If instead an electron in the $1a''$ orbital is removed, two singly occupied orbitals remain, and can couple to form a triplet and a singlet. The resulting cation of lower energy will be the triplet.

The $1a''$ orbital is π -like, analogous to the uppermost occupied $1b_{1u}$ orbital in ethylene. In C_2H_4 , the lowest energy process, corresponding to removal of an electron from the $1b_{1u}$ orbital, results in a cation with an increased C–C bond distance. The C–C bond distance in C_2H_4 is 1.339 Å²⁸, in the ${}^2B_{1u}$ state of $C_2H_4^+$, this distance has been determined to be 1.41 Å by Franck–Condon analysis of the photoelectron spectrum,²⁹ and by a Green's function *ab initio* calculation.³⁰ The C–H bond distance and the various angles do not change greatly, but there is evidence of twisting of the H_2C entities with respect to each other (and hence from planarity) by 16° – 18° .

Apart from this twisting motion, the major consequence of electron ejection from $1b_{1u}$ (i.e., the lengthening of the C–C bond) manifests itself in the photoelectron spectrum as a vibrational progression. One expects this vibrational progression to involve ν_2 , the C–C stretching mode, but in fact it involves ν_3 , the HCH bend, as well. As Botter and Carrier³¹ point out, this is a consequence of the strong mixing of the stretching and bending internal coordinates in the two nor-

TABLE IV. Calculated molecular geometries of (a) C_2H_3 in its ground ($^2A'$) state, and (b) $C_2H_3^+$ in its excited ($^3A''$) state.

	α	$R_{CC}, \text{\AA}$	$R_{C,H_1}, \text{\AA}$	$R_{C,H_2}, \text{\AA}$	$R_{C,H_3}, \text{\AA}$	β
H ^a (a)	120°	1.323	1.090	1.090	1.085	135°
CP-2 ^b (a)	116°	1.287	1.086	1.091	1.080	136.8°
CP-1 ^c (b)	118.9°	1.387	1.078	1.079	1.075	134.9°
CP-2 (b)	118.9°	1.395	1.0889	1.0918	1.0866	135.9°

^a H = Hunziker *et al.*, Ref. 18.

^b CP-2 = Curtiss and Pople, Ref. 12, MP2/6-31G*.

^c CP-1 = Curtiss and Pople, Ref. 12, HF/6-31G*.

mal modes ν_2 and ν_3 . At least three members of such a progression are readily detectable in the photoelectron spectrum of C_2H_4 .

Returning now to the C_2H_3 system, we list in Table IV the calculated structures of C_2H_3 in its ground ($^2A'$) state and $C_2H_3^+$ in its excited ($^3A''$) state, the latter resulting from removal of an electron from the $1a''$ orbital. As in the analogous case of C_2H_4 , the major effect of removing an electron from this π -bonding orbital is to increase the C–C distance. The calculations of Curtiss and Pople¹² imply an increase in this distance of ~ 0.10 – 0.11 Å, even larger than the 0.07 Å increase in ethylene. Hence, the corresponding photoelectron spectrum should manifest a progression in at least the C–C stretching vibration (~ 1375 cm^{-1} in $C_2H_4^+$), and at least three members of such a progression should be readily detectable. This same argument can now be extended to the Rydberg states converging on $C_2H_3^+$, $^3A''$, since their geometries should be close to the structure of the ionic state to which they converge.

The analogy we have drawn between the $1a''$ orbital in C_2H_3 and the $1b_{1u}$ orbital in C_2H_4 suggests that the ionization energies from these respective orbitals should be close to one another. The corresponding ionization potential in C_2H_4 is 10.51 eV. Hence, our analysis of the resonance structure in the photoion yield curve of C_2H_3 should anticipate Rydberg members converging to a limit of about 10.5 eV. Furthermore, each Rydberg member should have a vibrational progression of at least three members associated with it, having a vibrational spacing of roughly 1300 cm^{-1} .

We have tested several limits in the range 10.5–10.8 eV, with the above criteria in mind. No single solution is satisfactory. For assumed limits in the lower part of the range (10.5–10.6 eV), the observed peaks at high energy correspond to values of n^* which increase too abruptly. With a limit at 10.8 eV, they appear to increase too gradually. One possible solution, corresponding to a limit of 10.70 eV, is given in Table V. We have not been able to explore the possible fine structure within the peak features, due to the weak ion signal which limited our scan to the intense peaks in the light source. It is quite possible that more than one Rydberg series is involved.

For the corresponding excitation (from the $1b_{1u}$ orbi-

TABLE V. Tentative assignment of some of the autoionization resonances listed in Table III. (Assumed limit = 10.7 eV \equiv 86 300 cm^{-1} .)

$\lambda, \text{\AA}$	T_0, cm^{-1}	n^*	ν'
1316	75 988	3.26	0
1293	77 334		1
1271.6	78 644		2
1250	80 000	4.17	0
1234	81 037		1
1215.5	82 271	5.22	0,2 ^a
1208.8	82 727		1
1197.6	83 500	6.26	0
1188.3	84 157	7.16	0
1178.2	84 879		1 ^b

^a Dual assignment; $\nu' = 2$ refers to $\nu' = 0$ for the 1250 Å peak.

^b $\nu' = 1$ refers to $\nu' = 0$ for the 1179.6 Å peak.

tal) in C_2H_4 , Price and Tuttle³² found one strong Rydberg series, and two “much weaker” ones. Denoting the effective quantum numbers as $n^* = n + a$, their strong series corresponds to $a = 0.91$, the two weaker series with $a = 0.4$ and 0.7 . Wilkinson³³ has identified four Rydberg series; in the same notation, $a = 0.91, 0.4, 0.6,$ and 0.05 . The present data for C_2H_3 , as tentatively assigned in Table V, correspond to $a \approx 0.23$, which evidently does not match any of the values of “ a ” observed in ethylene.

Our ability to see autoionization structure obviously depends not only on the oscillator strengths of the absorbing bands, but also on the strength of the configuration interaction with the ionization continuum which results in autoionization. The studies on ethylene are photoabsorption measurements, dependent only on photoabsorption cross sections. It is possible that there exist in C_2H_3 Rydberg series with stronger photoabsorption cross sections, but with much weaker autoionizing probabilities.

B. C_2H_3 from pyrolysis of $(C_2H_3)_2Hg$

1. Photoionization mass spectrum of $(C_2H_3)_2Hg$ at room temperature

In order to establish the photon energy “window” where fragment $C_2H_3^+$ from photodissociative ionization will not interfere with primary photoionization of C_2H_3 , a cursory study was performed on the photoionization of divinyl mercury at room temperature. In Fig. 2, the photoion yield curves of $(C_2H_3)_2Hg^+$, $C_2H_3Hg^+$, and $C_2H_3^+$ from divinyl mercury are presented. The adiabatic ionization potential of divinyl mercury is found to be ~ 1395 Å \equiv 8.89 eV. Toward longer wavelength, the $C_2H_3^+$ fragment curve declines asymptotically to ~ 1100 Å, but it begins to increase significantly below ~ 1030 Å. Below ~ 960 Å, $C_2H_3^+$ is the dominant ion. Other ionic species observed with lower intensities include $m/e = 28$ ($C_2H_4^+?$), $m/e = 54$ ($C_4H_6^+?$), and $m/e = 39$ ($C_3H_3^+?$), possibly due to impurities in the sample. The wavelength region above ~ 1100 Å appears to be free from contamination by $C_2H_3^+$ due to dissociative photoionization of $(C_2H_3)_2Hg$. However, some contamination from the low mass tail of $m/e = 28$ appears to be present in the $C_2H_3^+$ photoion yield curve from pyrolyzed $(C_2H_3)_2Hg$, as will be seen below.

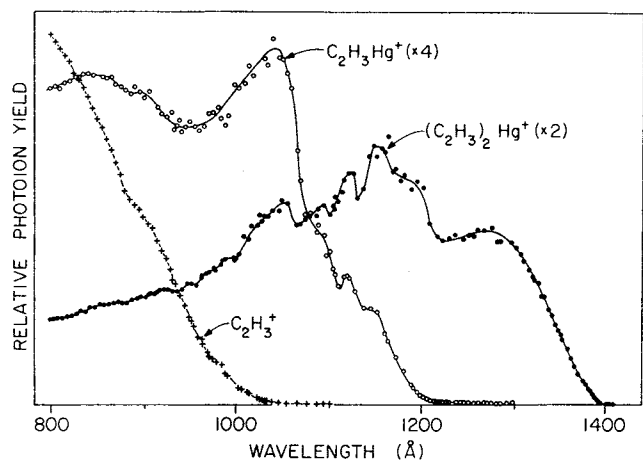


FIG. 2. Photoion yield curves of $(C_2H_3)_2Hg^+$, $C_2H_3Hg^+$, and $C_2H_3^+$ from divinyl mercury at room temperature.

2. Photoionization of C_2H_3 prepared by pyrolysis of $(C_2H_3)_2Hg$

From the studies described in Sec. III A, it was established that the strongest photoion signals for $C_2H_3^+$ (C_2H_3) occurred at 1217.35 and 1257.20 Å. These wavelengths combine strong light intensity with favorable photoionization cross sections, but do not necessarily correspond to maxima in the photoion yield curve. However, they are the most useful practical diagnostics, in our experiment, for monitoring the production of C_2H_3 .

The temperature of the pyrolysis reactor was gradually increased, and the $m/e = 27$ ion signal monitored at these two wavelengths. Optimum intensities were obtained at a temperature of $\sim 900^\circ C$, as measured by a Pt-Pt, 10% Rh thermocouple located in an annular region between the resistive heater and an inner tube through which the sample flowed. At this temperature, the parent ion, $(C_2H_3)_2Hg^+$, had diminished in intensity to $< 10\%$ of its value at room temperature, from which we conclude that $\sim 90\%$ of the sample was thermally decomposed. When steady state conditions were achieved at this temperature, a scan of $m/e = 27$ was performed at discrete wavelengths corresponding to light peaks. The resulting photoion yield curve is shown in Fig. 3.

The strong autoionization features observed when C_2H_3 was produced by the $F + C_2H_4$ reaction (Fig. 1) are seen to occur at about the same wavelengths in Fig. 3, although with somewhat different relative intensities. Both experiments require long counting times and assume a constant evolution of target C_2H_3 species, which is difficult to realize in practice, even with periodic renormalization at selected wavelengths. Hence, it is not too surprising that there may be variations in relative intensities at the autoionization resonances. However, both experiments (i.e., the F atom reaction and pyrolysis) were repeated, and rapid scans were made from peak to peak and in some valleys, and the relative intensities for each experiment were in reasonable accord. Therefore, some of the differences in peak intensities between Figs. 1 and 3, e.g., the peak at ~ 1215.5 Å, are believed to be real. The wavelengths of these resonances as determined in the pyrolysis experiment are also listed in Table III. At wave-

lengths shorter than 1180 Å, there is a gradual increase in the photoion yield curve, probably due to some "leakage" from $m/e = 28$.

The most significant difference between the photoion yield curve of Fig. 1 and that of Fig. 3 is the threshold region. In the pyrolysis experiment, a measurable photoion signal above the background level extends to ~ 1470 Å $\equiv 8.43$ eV, whereas the photoion yield curve of Fig. 1 seems to reach the background level at ~ 1450 Å $\equiv 8.55$ eV. Both results have been repeated, and we believe them to be significant. In addition, if we normalize to the intensity of the resonances nearest the threshold, the longer wavelength region is uniformly more intense in the pyrolysis experiment than in the $F + C_2H_4$ method of preparation.

C. Detailed examination of the threshold region

Several scans of the threshold region were performed, with both the chemical reaction method and the pyrolysis technique for generating C_2H_3 . A representative run of the $F + C_2H_4$ experiment is shown in Fig. 4(a), and one from the pyrolysis experiment in Fig. 4(b). The data span the region from 1400 to ~ 1520 Å, i.e., encompassing the onset and the background level. The smooth curve through each data set is a computer-generated spline fit. The two data sets have been normalized at ~ 1400 Å.

Clearly, the data set from pyrolysis-generated C_2H_3 [Fig. 4(b)] displays an onset at longer wavelength than the data set of Fig. 4(a). In both data sets, there is a region which

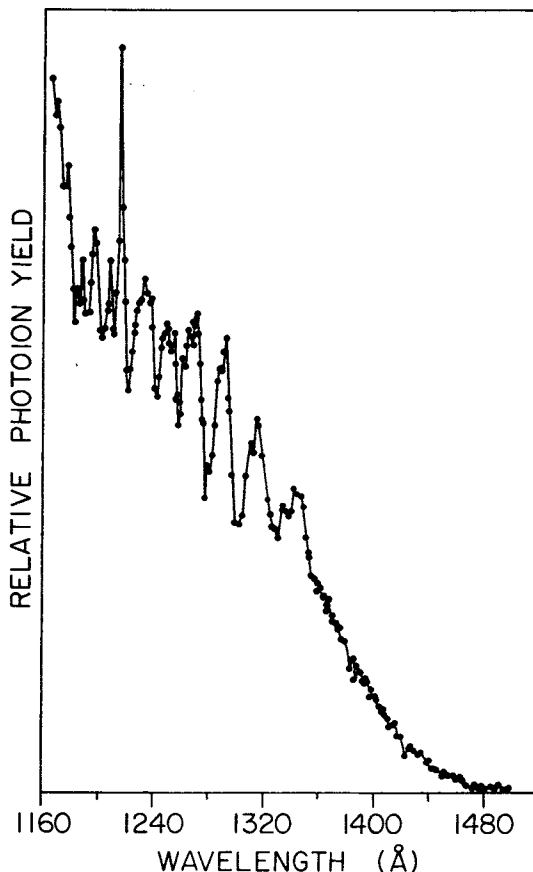


FIG. 3. Overview spectrum of the photoion yield of $C_2H_3^+$ (C_2H_3), where C_2H_3 is prepared by pyrolysis of divinyl mercury at $\sim 900^\circ C$.

displays a linear decline to the background level. The intersection of this linearly descending region with the background occurs at $\sim 1448 \text{ \AA} \equiv 8.56 \text{ eV}$ in Fig. 4(a), and at $\sim 1476 \text{ \AA} \equiv 8.40 \text{ eV}$ in Fig. 4(b). This characteristic difference between the pyrolysis and chemical reaction experiments can be noted in every pair of data sets.

In addition, there are indications of step-function behavior in both photoion yield curves. If this is indeed the case, it indicates that direct ionization, rather than autoionization, is the prevailing mechanism. Since there are Rydberg states converging to this lowest ionization potential, they must then be predominantly predissociating, which would make the quantum yield of ionization small at threshold. If direct ionization is the dominant feature, then the steps involve one or more vibrational progressions governed by Franck–Condon factors connecting the vinyl radical and ground state vinyl cation. To exploit this possibility, we have differentiated the smooth, spline-fitted curves in each of the data sets, from threshold to $\sim 1360 \text{ \AA} \equiv 9.1 \text{ eV}$. If rounded step-function behavior is indeed present in the photoion yield curve, then the derivative should display a pattern similar to a photoelectron spectrum. The rounded steps could be attributed to rotational effects. Both the chemical reaction and pyrolysis experiments display peaks which occur at 8.98, 8.86, 8.74, and 8.62 eV. These are averaged values from several experiments, but the uncertainty is $\leq 0.02 \text{ eV}$. In addition, the pyrolysis data reveal an additional, lower energy peak at 8.46 eV. The difference between the lowest energy peak in the pyrolysis experiment and the lowest energy peak in the $F + C_2H_4$ experiment is 0.16 eV, the same as that obtained from the difference in extrapolated thresholds of Figs. 4(a) and 4(b). The offset between the positions of the derivative peaks (8.46 and 8.62 eV) and the extrapolated thresholds (8.40 and 8.56 eV) is a measure of the peak widths.

The peak features common to both experiments appear to display a vibrational progression, the successive peaks differing in energy by $0.12 \text{ eV} \equiv 965\text{--}970 \text{ cm}^{-1}$. If we seek to interpret this pattern, we must examine the most likely normal modes of vinyl cation that will be excited in the ionizing transition. Such a normal mode should be totally symmetric with respect to all symmetry operations that apply to both the geometry of the initial and final states, and the internal coordinates describing this mode should reflect the change in geometry that has occurred when vinyl radical becomes vinyl cation. Vinyl radical has C_s symmetry, with in-plane a' totally symmetric modes and out-of-plane a'' non-totally symmetric modes. The vinyl cation, in either the classical or nonclassical structure, has C_{2v} symmetry. In-plane, totally symmetric modes a_1 retain C_{2v} symmetry, and hence cannot reflect the geometric change occurring when vinyl radical becomes vinyl cation. Hence, we eliminate a_1 modes from consideration, and also a_2 and b_1 modes (out-of-plane). This leaves only b_2 modes.

Both Raine and Schaeffer³⁴ and DeFrees and McLean³⁵ have computed the normal mode frequencies of $C_2H_3^+$ from their respective *ab initio* calculations, for both the classical and nonclassical forms. For both structures, there are three normal modes of b_2 symmetry (b_1 in Raine and Schaeffer's

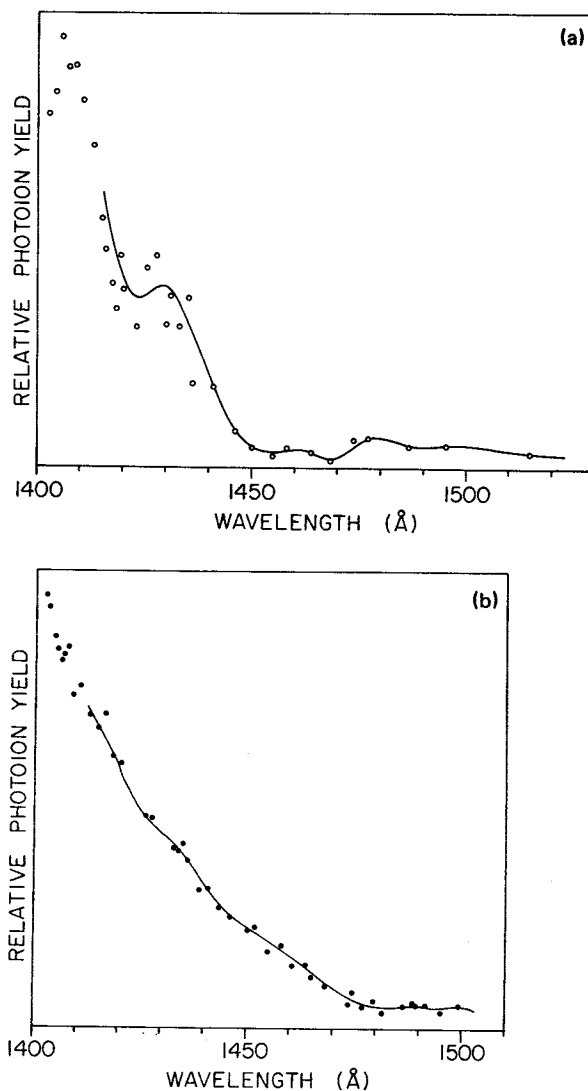


FIG. 4. (a) Threshold region of the photoion yield curve of $C_2H_3^+$ (C_2H_3); C_2H_3 prepared by the $F + C_2H_4$ reaction. (b) Threshold region of the photoion yield curve of $C_2H_3^+$ (C_2H_3); C_2H_3 prepared by pyrolysis of divinyl mercury. The smooth curves through the data points are computer-generated spline fits.

convention). Of these three modes, one is a C–H stretch in both classical and nonclassical structures which has a high frequency ($> 3000 \text{ cm}^{-1}$) and does not reflect the change of geometry between radical and cation. The remaining b_2 modes have calculated frequencies of 481/517 and 1166/1179 cm^{-1} (Raine/DeFrees) for the classical structure, 379/332 and 1323/1357 cm^{-1} for the nonclassical structure. (These are unscaled Hartree–Fock values. Better agreement with experiment is often obtained by multiplying the calculated value by 0.89.) Roughly, the higher frequencies correspond to eigenvectors¹² which relate to the geometric change between radical and cation, whereas the lower frequencies are characterized by eigenvectors¹² describing the change between classical and nonclassical ion structures.

The spacing in derivative peaks inferred from our experimental data could conceivably be identified with the higher frequency b_2 modes in either of these ionic structures, although it is closer to the classical structure. However, the

consensus of the best *ab initio* calculations (see Table II) suggests a more complicated interpretation. The calculated difference between the minima of both structures is $\sim 3\text{--}4$ kcal/mol, which is of the order of one vibrational quantum. The barrier between structures is calculated to be at most 1 kcal/mol. Hence, the potential surface of the vinyl cation may be crudely represented by the sketch in Fig. 5, in which the abscissa is the coordinate of the C–H in-plane bending mode. A more precise interpretation of the photoelectron spectrum (or pseudophotoelectron spectrum) must therefore await an accurate calculation of the Franck–Condon factors connecting the potential surface of vinyl radical with the rather complex potential surface of vinyl cation.

When such a calculation becomes available, it may be possible to deduce whether the current experiment is sensitive enough to detect the true adiabatic ionization potential. For the moment, we can draw the following tentative conclusions.

(1) The lower threshold observed in the pyrolysis experiment is almost certainly a hot band. The lowering in energy amounts to $\sim 1300\text{ cm}^{-1}$. The Boltzmann population of such a vibrational excitation at $\sim 1200\text{ K}$ (either as $v'' = 1$ of a 1300 cm^{-1} quantum or $v'' = 2$ of a 650 cm^{-1} vibration) is about 20%. However, the “step height” at the threshold in Fig. 4(b) ($\sim 1470\text{ \AA}$) can be expected to be more than 20% of the step height at $\sim 1445\text{ \AA}$, because the corresponding Franck–Condon factor should be larger. One can anticipate a rough symmetry in Franck–Condon factors between $0 \rightarrow 1$ and $1 \rightarrow 0$, $1 \rightarrow 2$ and $2 \rightarrow 1$, etc. The step height at $\sim 1425\text{ \AA}$ is about twice that at $\sim 1445\text{ \AA}$ in Fig. 4(a). Applying this same factor, the step height at $\sim 1470\text{ \AA}$ should be about 40% of that at $\sim 1445\text{ \AA}$ in Fig. 4(b), and it closely approximates that relative intensity. By contrast, if the $F + C_2H_4$ reaction produces C_2H_3 corresponding to room temperature as we believe, the Boltzmann population of a 1300 cm^{-1} excitation is $< 0.2\%$.

(2) An upper limit to the adiabatic ionization potential of vinyl radical can be obtained from Fig. 4(a), the “cold” C_2H_3 . The extrapolated threshold is 8.56 eV; the peak in the derivative spectrum is at 8.62 eV. The rotational $0 \rightarrow 0$ transition for this vibrational transition probably lies between these values.

IV. DISCUSSION

A. Implications of the threshold for the C–H bond energy

The best current value for the appearance potential of $C_2H_3^+$ in reaction (2) is $13.22 \pm 0.02\text{ eV}$, which appears to be very close to the true thermochemical threshold.

Our upper limit to the adiabatic ionization potential of C_2H_3 is $8.59 \pm 0.03\text{ eV}$. When combined with the appearance potential of reaction (2), this yields a *lower* limit to the C–H bond energy in ethylene of $4.63 \pm 0.04\text{ eV} \equiv 106.8 \pm 0.8\text{ kcal/mol}$ at 0 K. Recently, Curtiss and Pople¹² have calculated an adiabatic ionization potential for C_2H_3 (going to the nonclassical bridged structure) of 8.42 eV. Typically, those recent calculations have been accurate to $\pm 0.1\text{ eV}$. Thus, it is quite possible that the vibrational

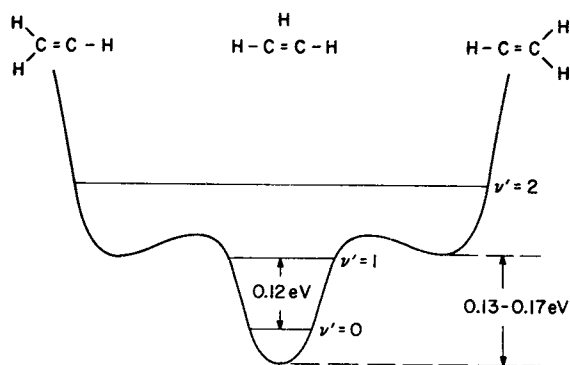


FIG. 5. A schematic sketch of the potential energy surface of vinyl cation in its ground state, with the amplitude of the in-plane C–H bending motion as the abscissa.

$0 \rightarrow 0$ transition, corresponding to formation of vinyl cation in a bridged structure very different in geometry from the vinyl radical, has such a low Franck–Condon factor that it is not detected in our experiment. In effect, it may mean that our threshold is one vibrational quantum shy of the true threshold. If the true threshold is lower by such an amount, the C–H bond energy in ethylene becomes 110 kcal/mol. The recent calculations by Curtiss and Pople¹² give $110.2 \pm 2\text{ kcal/mol}$ for this quantity.

In summary, the low value of $\sim 100\text{ kcal/mol}$ for the C–H bond energy in ethylene is definitely ruled out by our experimental results. They indicate a value of at least 107 kcal/mol, and perhaps as high as 110 kcal/mol. A value of 117 kcal/mol, while not definitively ruled out by the present experiments, seems highly unlikely. A more precise statement awaits calculation of the relevant Franck–Condon factors.

B. The energies and structures of vinyl cation

The adiabatic ionization potential of C_2H_3 obtained in the present experiment, $\leq 8.59 \pm 0.03\text{ eV}$, is considerably lower than the best previous value,⁹ 8.95 eV, obtained by electron impact. The low photoion yield near threshold implies a large geometry change.

By contrast, the relatively sharp autoionization structure observed at higher energy, and its interpretation, lead us to the conclusion that the first excited state, a triplet, has a structure rather similar to that of vinyl radical, but with a larger C–C distance.

The structure of the ground state of vinyl cation remains a bit fuzzy. Oka's²¹ partial analysis of the infrared spectrum convinces him that the nonclassical structure dominates, but that the spectrum is not that of a usual well-behaved asymmetric rotor. The extensive calculations summarized in Table I predict that the classical structure lies just 3–4 kcal/mol above the nonclassical structure, with a barrier between structures of at most 1 kcal/mol. The “Coulomb explosion” experiments²² were performed on $C_2H_3^+$ prepared by “low-energy electron bombardment of ethylene.” We know from the photoionization studies of ethylene that the $C_2H_3^+$ fragment increases in abundance rather slowly from threshold. This gradual increase is likely to occur in electron impact experiments as well. Hence, to achieve a measurable signal,

one must exceed the threshold energy by perhaps 1 eV. Usually, such electron impact experiments have significant energy spreads, ± 0.3 – 0.5 eV, unless an electron monochromator is used. The $C_2H_3^+$ initially formed by electron bombardment of C_2H_4 is likely to be "hot", i.e., to encompass some vibrational distribution in addition to the vibrational ground state. If the *ab initio* calculations are to be relied upon, $C_2H_3^+$ species having an internal energy of only 0.5 eV will already vibrate in a potential surface that includes both classical and nonclassical structures. The Coulomb explosion experimentalists note²² that with their method "it is possible to obtain average geometries directly". If the $C_2H_3^+$ they are examining is mildly hot vibrationally, and both classical and nonclassical structures are represented in their sample, it may still be possible that the *average* positions of the protons which they observe will conform to the nonclassical structure.

ACKNOWLEDGMENTS

This research was supported by the Department of Energy (Office of Basic Energy Sciences) under contract W-31-109-ENG-38 and by the U.S.–Yugoslav Joint Board for Science and Technology through the U.S. Department of Energy Grant No. PN 561.

¹M. W. Chase, Jr., C. A. Davies, J. R. Downey, Jr., D. J. Frurip, R. A. McDonald, and A. N. Syverud, *JANAF Thermochemical Tables*, 3rd ed. (American Chemical Society, Washington, D.C., 1985), Vol. 14 of J. Phys. Chem. Ref. Data, Suppl. No. 1.

²H. Shiromaru, Y. Achiba, K. Kimura, and Y. T. Lee, *J. Phys. Chem.* **91**, 17 (1987).

³R. Botter, V. H. Dibeler, J. A. Walker, and H. M. Rosenstock, *J. Chem. Phys.* **45**, 1298 (1966).

⁴W. A. Chupka, J. Berkowitz, and K. M. A. Refaey, *J. Chem. Phys.* **50**, 1938 (1969).

⁵R. Stockbauer and M. G. Inghram, *J. Chem. Phys.* **62**, 4862 (1975).

⁶D. Reinke, R. Kraessig, and H. Baumgartel, *Z. Naturforsch. Teil A* **28**, 1021 (1973).

⁷V. P. Glushko, L. V. Gurvich, G. A. Bergman, I. V. Veits, V. A. Medvedev, G. A. Khackhunuzov, and V. S. Yungman, *Termodinamicheski Svoistva Individual'nikh Veschestv* (Nauka, Moscow, 1979), Vol. 2.

⁸A. G. Harrison and F. P. Lossing, *J. Am. Chem. Soc.* **82**, 519 (1960).

⁹F. P. Lossing, *Can. J. Chem.* **49**, 357 (1971).

¹⁰H. M. Rosenstock, K. Draxl, B. W. Steiner, and J. T. Herron, *J. Phys. Chem. Ref. Data* **6**, Suppl. 1, I-96 (1977).

¹¹R. Lindh, B. O. Roos, and W. P. Kraemer, *Chem. Phys. Lett.* **139**, 407 (1987).

¹²L. A. Curtiss and J. A. Pople, *J. Chem. Phys.* **88**, 7405 (1988).

¹³J. Berkowitz, *Photoabsorption, Photoionization, and Photoelectron Spectroscopy* (Academic, New York, 1979).

¹⁴D. F. McMillen and D. M. Golden, *Annu. Rev. Phys. Chem.* **33**, 493 (1982).

¹⁵J. H. Kieffer, H. C. Wei, R. D. Kern, and C. H. Wu, *Int. J. Chem. Kinet.* **17**, 225 (1985).

¹⁶G. B. Ellison (private communication).

¹⁷C. H. DePuy, V. M. Bierbaum, and R. Damrauer, *J. Am. Chem. Soc.* **106**, 4051 (1984).

¹⁸H. E. Hunziker, H. Knepe, A. D. McLean, P. Siegbahn, and H. R. Wendt, *Can. J. Chem.* **61**, 993 (1983).

¹⁹T. J. Lee and H. F. Schaeffer III, *J. Chem. Phys.* **85**, 3437 (1986).

²⁰J. A. Pople, *Chem. Phys. Lett.* **137**, 10 (1987).

²¹T. Oka, *Philos. Trans. R. Soc. London Ser. A* **324**, 81 (1988).

²²E. P. Kanter, Z. Vager, G. Both, and D. Zajfman, *J. Chem. Phys.* **85**, 7487 (1986).

²³(a) S. T. Gibson, J. P. Greene, and J. Berkowitz, *J. Chem. Phys.* **83**, 4319 (1985); (b) J. Berkowitz, J. P. Greene, H. Cho, and B. Rušćić, *J. Chem. Phys.* **86**, 1235 (1987).

²⁴J. M. Parson and Y. T. Lee, *J. Chem. Phys.* **56**, 4658 (1972).

²⁵I. R. Slagle and D. Gutman, *J. Phys. Chem.* **87**, 1818 (1983).

²⁶D. J. Bogan and D. W. Setser, *J. Chem. Phys.* **64**, 586 (1976).

²⁷J. Berkowitz, L. A. Curtiss, S. T. Gibson, J. P. Greene, G. L. Hillhouse, and J. A. Pople, *J. Chem. Phys.* **84**, 375 (1986).

²⁸J. L. Duncan, J. J. Wright, and D. Van Leberghe, *J. Mol. Spectrosc.* **45**, 221 (1973).

²⁹J. Carlier and R. Botter, *J. Chim. Phys.* **81**, 371 (1984).

³⁰H. Koppel, W. Domcke, L. S. Cederbaum, and W. von Niessen, *J. Chem. Phys.* **69**, 4252 (1978).

³¹R. Botter and J. Carlier, in *Ionic Processes in the Gas Phase*, edited by M. A. Almoester-Ferreira (Reidel, Dordrecht, 1984), pp. 303–325.

³²W. C. Price and W. T. Tutte, *Proc. R. Soc. London Ser. A* **174**, 207 (1940).

³³P. G. Wilkinson, *Can. J. Phys.* **34**, 643 (1956).

³⁴G. P. Raine and H. F. Schaeffer III, *J. Chem. Phys.* **81**, 4034 (1984).

³⁵D. J. DeFrees and A. D. McLean, *J. Chem. Phys.* **82**, 333 (1985).